

Chimeric Virus-Like Particles Made Using GAG and M1 Capsid Proteins Providing Dual Drug Delivery and Vaccination Platform

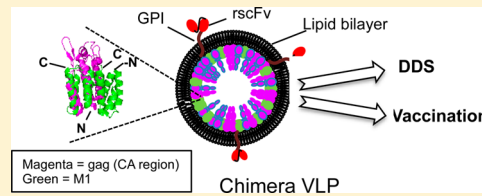
Vipin K. Deo,[†] Tatsuya Kato,[‡] and Enoch Y. Park*,^{†,‡}

[†]Laboratory of Biotechnology, Integrated Bioscience Section, Graduate School of Science and Technology, [‡]Laboratory of Biotechnology, Research Institute of Green Science and Technology, Shizuoka University, 836 Ohya, Suruga-ku, Shizuoka 422-8529, Japan

 Supporting Information

ABSTRACT: Nanobiomaterials such as enveloped virus-like particles with specificity can serve a dual function of vaccination and drug delivery system. Here, we expressed colon carcinoma cell-targeting chimeric virus-like particles (VLPs) made using two capsid proteins, gag and M1 from influenza virus A/swine flu/Iowa/15/30/H1N1 in silkworms. These chimeric VLPs displayed a glycosylphosphatidylinositol-anchored single-chain variable fragment region targeting colon carcinoma cells, and their shape was smooth, with an average particle size of 21 nm in diameter. Large unilamellar vesicles made from DOPC:DOPA (2:1) containing calcein-AM (10 μ M) or doxorubicin (13.7 nM) were used to package chimeric VLPs. VLPs showed high specificity in targeting cancer cells and delivered the dye and drug to cells successfully. Chimeric VLPs were injected into BALB/c mice, and the serum showed specificity for M1 protein as a model.

KEYWORDS: virus-like particles, drug delivery system, vaccination, chimeric, silkworm expression system



INTRODUCTION

Different types of virus-like particles (VLPs) can be produced using virus capsid protein, which self-assembles to form VLPs. The VLPs are devoid of any genetic material, and they provide useful information for viral infection mechanisms and also serve as a very effective tool for vaccination.^{1,2} There are many types of capsid proteins, but here, the primary focus was on lipid layer-surrounded VLPs, because the lipid surface can be used to display proteins for functionalization with ease.³ VLP formation has been well studied and is due to the aggregation of monomers on the plasma membrane, causing a change in surface tension and leading to budding of VLPs by subsequent pinching.^{4–6} Most of the physical characteristic features of VLPs, such as size and shape, are affected by the presence of displayed proteins or the selected capsid protein. Larger proteins, when displayed on the surface of VLPs, usually form VLPs of larger diameter.^{7,8} We have already shown that group antigen protein (gag) from *Rous sarcoma* virus belonging to the retrovirus family can form VLPs with a lipid bilayer with ease when expressed in silkworms using the bacmid expression system.^{7–9}

Here, the feasibility of coexpressing two capsid proteins and their ability to form VLPs, henceforth referred to as chimeric VLPs or chimeras, was explored. Chimeric VLPs using the coexpression method has been reported earlier, and here we used a similar method to produce chimera using two different coat proteins.^{10,11} Such nanobiomaterial can be a useful tool with dual function for vaccination and as a novel drug delivery system (DDS). Multifunctional biomaterials can serve as immunogens against different infections and be beneficial in preventing cross-infection from different sources with ther-

apeutic properties for fast recovery.^{12,13} As a model, targeting of colon carcinoma cancer and vaccination against influenza viral infection using chimeric VLPs is reported here. There is no effective drug targeting colon carcinoma without harmful side effects, often leading to discomfort and excruciating pain.^{14,15} The nanobiomaterial reported here fits the established paradigm for DDS of using known chemotherapeutic agents combined with novel target delivery systems to specifically deliver on site, thus reducing side effects, needed for fast and effective recovery.^{16–22}

Here, chimeric VLPs were prepared using gag and M1 capsid proteins; they have a common modus operandi, wherein they first enter the nucleus and interact with RNA and then proceed further toward the plasma membrane.²³ M1 is a well-known and highly conserved capsid protein in the influenza virus family. Various M1, M1-hemagglutinin (HA), M1-HA-neuraminidase (NA) combinations have been tried with varying results, and yet, no definite vaccine using M1 is available.^{1,24–27} The reason is because M1 requires interaction with the cytoplasmic tail region of other proteins such as HA, NA, and M2 to direct it toward the plasma membrane to form the VLPs.²⁶ However, gag proteins do not require any assistance to form VLPs, because they are self-sufficient and use the host cell protease for final processing of VLPs. The merit of using VLPs is that they are known to present the antigens effectively without the use of any adjuvants, thus serving as an ideal

Received: October 2, 2014

Revised: January 24, 2015

Accepted: January 27, 2015

Published: January 27, 2015

vaccination platform.^{8,28} We are also interested in the shape and size of novel biomaterial, which are related to their ability to be used as a nanoscale DDS platform.²² It has been observed that nanocarriers easily diffuse through physical membrane barriers with higher penetration of the target.

Here we propose that a chimera made using gag and M1 capsid proteins, both known to aggregate on the plasma membrane when coexpressed in the silkworms using *Bombyx mori* nucleopolyhedrovirus (BmNPV), can produce nanoscale macromolecular structures. The remarkable point of this approach is that the capsid proteins are not tagged or fused, thus eliminating the chance of modifications in antigenic surface. As a result, the native form is retained, and the advantage of displaying other proteins on its lipid surface allows the chimeric VLPs to have dual functions for both drug delivery and vaccination. Here, we found that chimeric VLPs displayed a single-chain variable fragment region (rscFvs) which targets tumor-associated glycoprotein-72 (TAG-72), a known colon carcinoma marker on chimeric VLPs. The display of rscFvs on chimeric VLPs provides the homing ability of the nano-biomaterial. The silkworm expression system has been reported to produce VLPs effectively, and here, it was used to develop chimeric VLPs, using a similar expression system which is easy to scale up.^{7–9,29}

EXPERIMENTAL SECTION

Expression of Chimeric VLPs in Silkworm, Purification, and Confirmation. Influenza A/swine/Iowa/15/30 virus RNA (ATCC VR-1683D) was used to perform reverse transcription PCR using oligo dTs as per the kit protocol (Takara Bio, Otsu, Japan). M1 cDNA was synthesized using PCR primers (Table 1) and ligated into pFastBac vector by the

Table 1. List of Primers Used To Synthesize M1 cDNA

name	5' to 3'
forward primer for M1	GAAGCGCGGAAATTATGAGCCTCTAACCGAAGTC
reverse primer for M1	TACCGCATGCCCTCGATCACTTGAATCGTTGCATCTG
pfastbac vector forward primer	TCGAGGCATCGGTACCAAGCTTGTGAG
pfastbac vector reverse primer	AATTCCGCGCGCTTCGGACCGGGATC

infusion method (Takara Bio, Otsu, Japan). The recombinant bacmid carrying M1 was isolated and purified as other recombinant bacmid carrying gag-577 and rscFvs (glycosyl-phosphatidylinositol [GPI]-anchored single-chain variable fragment regions) as previously described.^{7,28} Silkworm larvae were reared and fed as reported earlier,^{8,9} and they were injected with 40 μL of recombinant bacmid DNA solutions containing 5 μg of BmNPV-gag577,⁸ 5 μg of BmNPV-scFv-GPI⁸ or 5 μg of BmNPV-M1 bacmids, in 10% (v/v) DMRIE-C reagent (Invitrogen) in PBS, using a 1 mL syringe with 26G × 1/2 in. needle (Terumo, Somerset, NJ, U.S.A.).

Larval hemolymph collected from silkworms was used for purification of chimeric VLPs, and the presence of M1, GP64, rscFvs, and gag-577 of purified chimeric VLPs was confirmed by Western blotting using (Supporting Information No. 1). The antigen specificity and GPI anchoring of chimeric VLPs were confirmed (Supporting Information No. 2).

The amount of M1 present on the chimeric VLPs per microgram was estimated by analyzing band intensity of Western blots using Quantity One software (Bio-Rad). Standard was prepared using purified M1 (H1N1 A/Puerto Rico/8/34/Mount Sinai) protein (Sino Biological Inc., China) because a commercial source of swine (H1N1 A/Iowa/15/30) M1 was not available. High nucleotide homology (94%) of M1 protein from the two viral strains was confirmed. M1 standards ranging from 150 to 37.5 ng were prepared. Like for the chimera bands, the intensity was calculated and compared with standards.

Chimera-rscFvs Specificity for LS174T Cells. LS174T and HEK293 cell lines were obtained as reported earlier and cultured for 3 days; around 10⁴ cells were seeded on 4-chamber glass slides (SPL Life Sciences Ltd, Pocheon-city, Gyeonggi-do, South Korea) and incubated overnight under growing conditions.²⁹ The cells were washed with fresh medium and incubated with 5 μg of chimeric VLPs for 3 h. The cells in each chamber were treated with 500-fold diluted BODIPY FL-C5-ceramide conjugated to BSA (Invitrogen). The cells were then probed with 1000-fold diluted anti-DYKDDDDK-tag-Alexa Fluor 594 (MBL Co. Ltd., Nagoya, Aichi, Japan) for rscFvs, rabbit anti-RSV-gag primary antibody for gag-577,⁹ or polyclonal rabbit anti-M1 for influenza A virus M1 (A/Puerto Rico/8/1934 [H1N1]) (GeneTex, Irvine, CA, U.S.A.) and incubated for 1 h at 37 °C. The cells probed for gag and M1 were then washed with fresh growth medium and incubated with 2000-fold diluted goat antirabbit IgG (H+L) conjugated to Alexa Fluor 647 (Santa Cruz Biotechnology). The cells were then washed with fresh growth medium and incubated with 1000-fold diluted 4'-6-diamidino-2-phenylindole hydrochloride (DAPI) solution (Dojindo) for 1 h at 37 °C. The cells were washed once, fixed with 2% (v/v) formaldehyde (Wako Pure Chemical Industries, Ltd., Osaka, Japan) and viewed under a confocal laser scanning microscope (CLSM) (LSM 700, Carl Zeiss, Oberkochen, Germany) with plan-apochromatic 40× oil immersion lens. Zen LE software available on Carl Zeiss Web site was used for image analysis.

Delivery of Calcein-AM to LS174T Cells. LS174T cells as mentioned above were cultured and seeded onto the slides. The cells were washed with fresh medium and incubated with 5 μg of chimeric VLPs-calcein-AM, 100 μL of large unilamellar vesicle (LUV)-calcein-AM (Supporting Information No. 3) as a negative control for 3 h. The cells were washed and treated with 1000-fold diluted mouse monoclonal anti-DDDDK and incubated for 1 h at 37 °C. The cells were washed and treated with 2000-fold diluted A647 conjugated goat antimouse IgG (H+L) (Jackson ImmunoResearch Lab., Baltimore, MD, USA) and incubated for 1 h at 37 °C. The cells were washed once, fixed with 2% (v/v) formaldehyde, and viewed under CLSM with plan-apochromatic 63× oil immersion lens. Zen LE software available on Carl Zeiss Web site was used for image analysis.

Spheroid Preparation and DDS Experiments. The spheroids were used as a model for solid tumors of 100 μm in diameter, prepared using micro molds for casting 3D Petri dishes (MicroTissues Inc., Providence, RI, U.S.A.) using LS174T cells.^{27,29} One hundred micrograms of chimera VLPs in 500 μL of HEPES (pH7.5) buffer were mixed with 500 μL of LUV-calcein-AM or LUV-doxorubicin, and incubated for 1 h at 27 °C for fusion to be complete. The complete mixture was added to the spheroids, which were then incubated for 3 h at 37 °C under optimum cell growing conditions. Following

incubation, the spheroids were washed thrice with fresh growth medium, treated with 250-fold diluted mouse monoclonal anti-DDDDK in 500 μ L of growth medium, and incubated at 37 °C in a CO₂ incubator for 1 h. The spheroids were washed with fresh growth medium, treated with 500-fold diluted goat antimouse IgG (H+L) conjugated with A647 (Jackson ImmunoResearch Lab.) in 500 μ L of growth medium, and incubated at 37 °C in CO₂ incubator for 1 h. The spheroids were washed with fresh growth medium and viewed under CLSM under live conditions with a 10× apochromatic lens. The penetration of dyes and drugs in the spheroids was observed by taking Z-stacked images of spheroids with cross-sectional scanned layers of 1 μ m. All Z-stacked images collected were rendered to prepare the 3D model using Zen LE 2011 version software available on Carl Zeiss Web site.

Mouse Immunization and Mouse Serum Specificity for Chimeric VLPs. Five female BALB/c mice were used for immunization and confirmation of mouse serum specificity for chimeric VLPs (Supporting Information No. 4).

RESULTS

Chimeric VLP Purification and Confirmation of rscFvs. Chimeric VLPs were expressed in silkworms, and larval hemolymph was collected, which was used for purification using DDDDK-tagged protein purification gel. Chimeras displayed rscFvs with FLAG tag at the N-terminal end and a GPI site at C-terminal end for anchoring on the lipid surface. Chimeric VLPs were composed of gag (61 kDa), M1 (28 kDa), glycoprotein 64 GP64 (64 kDa), and rscFvs (32 kDa), and the presence of all proteins was confirmed by Western blotting (Figure S1 A–D). For M1 protein, a few other bands were observed, which might have been due to the polyclonal antibody nonspecificity as observed for negative control using hemolymph only (Figure S1 E). The purification of the chimeric VLPs was aided by FLAG-tagged rscFvs, because gag and M1 have no tags. Coomassie blue staining showed the presence of all components of chimeric VLPs (Figure S1 F). The amount of M1 present on the chimeric VLPs per microgram was estimated to be 305 ng, which was about 30.5% of total chimera protein.

Here, we used DOPC/DOPA (2:1 ratio)-derived LUVs, because it has been reported that the presence of 50% acidic lipid (DOPA) in LUVs facilitates GP64-assisted fusion.³⁰ The function of rscFvs was confirmed by using antigen binding affinity of rscFvs for TAG-72 by ELISA (Figure 1A). rscFvs was anchored on chimeric VLPs by GPI anchor, and this was confirmed by enzymatic cleavage of the phosphodiester linkage by PI–PLC by ELISA (Figure 1B). Thus, a functional and anchored rscFvs on chimera targeting TAG-72 was confirmed.

Specificity and Structural Characteristics of Chimeric VLPs. Chimeric VLPs showed specificity for the LS174T cells displaying TAG-72, a known marker for colon carcinoma (Figure 2) compared with HEK293T cells as negative control (Figure S2). The CLSM images of LS174T cells showed the presence of all the components of chimeric VLPs: gag, M1, and rscFvs (Figure 2C, G, and K). The exact ratio of gag and M1 proteins necessary to form chimeric VLPs is still unknown. The structural morphology of chimeric VLPs was confirmed by TEM (Figure 3A) and was found to be smooth. The presence of 2–3 particles of rscFvs per chimera were confirmed by immuno-TEM (Figure 3B). The structural morphology was more or less similar to gag-577 based VLPs, as reported earlier with the only difference being in diameter.^{7–9,29} The

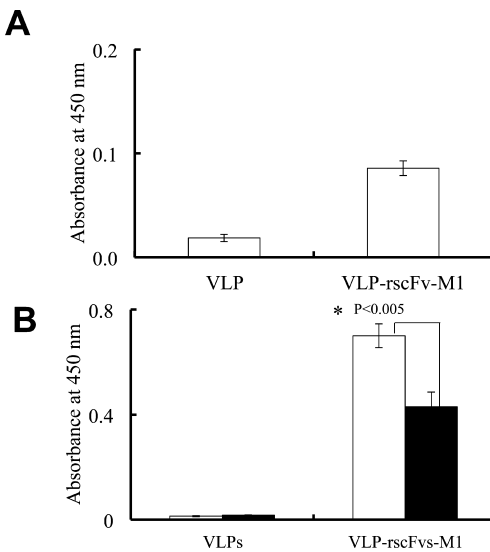


Figure 1. (A) ELISA to confirm the specificity and anchoring of rscFvs on purified chimeric VLPs for TAG-72. (B) Confirmation of the GPI anchor by PI–PLC enzymatic digestion. Black box: with PI–PLC, White box: without PI–PLC. Data are the mean \pm SD ($n = 3$).

quantitative analysis of the size of the chimeric VLPs (median peak of 21 nm), VLPs (median peak of 50.75 nm), and VLP-rscFvs (median peak of 105.7 nm) was performed using dynamic light scattering using Malvern Zetasizer software, and a decrease in diameter was observed for chimeric VLPs (Figure 3C).

Testing DDS Model. Chimeric VLPs were packaged using LUVs packaged with 10 μ M calcein-AM or 13.7 nM doxorubicin at room temperature and pH 7.5. Calcein-AM is well suited to study drug delivery as it produces fluorescence only when inside the cell due to cellular esterase activity. LS174T cells when treated with chimeric VLPs packaged with calcein-AM showed fluorescence (Figure 4A–D). The fluorescence of calcein-AM along with the presence of gag signifies the delivery by chimeric VLPs. As a negative control, the cells without any packaged chimeric VLPs but with similar amount of LUV-calcein-AM used for packaging showed no fluorescence for both gag and calcein-AM (Figure 4E–H).

Chimeric VLPs can be used for DDS applications owing to their small size and colon cancer-targeting specificity. Spheroids ranging from 10–500 μ m have been used in an in vitro model for colon cancer tumor.²⁵ We have previously shown that large spheroids can be easily prepared and used as a model to study dye penetration using VLPs.²⁹ Large spheroids (Figure S3) were treated with 100 μ g of chimeric VLPs packaged with similar amounts of calcein-AM as mentioned above. The delivery of dye (red channel) was confirmed along with the presence of displayed rscFvs fluorescence (green channel) targeting the tumor-specific marker (TAG-72) (Figure 5A,B). The overlapped images showed the presence of both channels (yellow color) (Figure 5C), indicating the potential of chimeric VLPs as a DDS platform. The DDS model was further tested by packaging chimeric VLPs with doxorubicin a known effective chemotherapeutic reagent that intercalates DNA.^{19,31} The delivery of doxorubicin to spheroids was confirmed (red channel) along with the presence of rscFvs fluorescence (green channel) (Figure 5D,E). The overlapped images showed the presence of both channels and confirmed the delivery of drug (Figure 5F). Thus, chimeric VLPs based on the DDS model

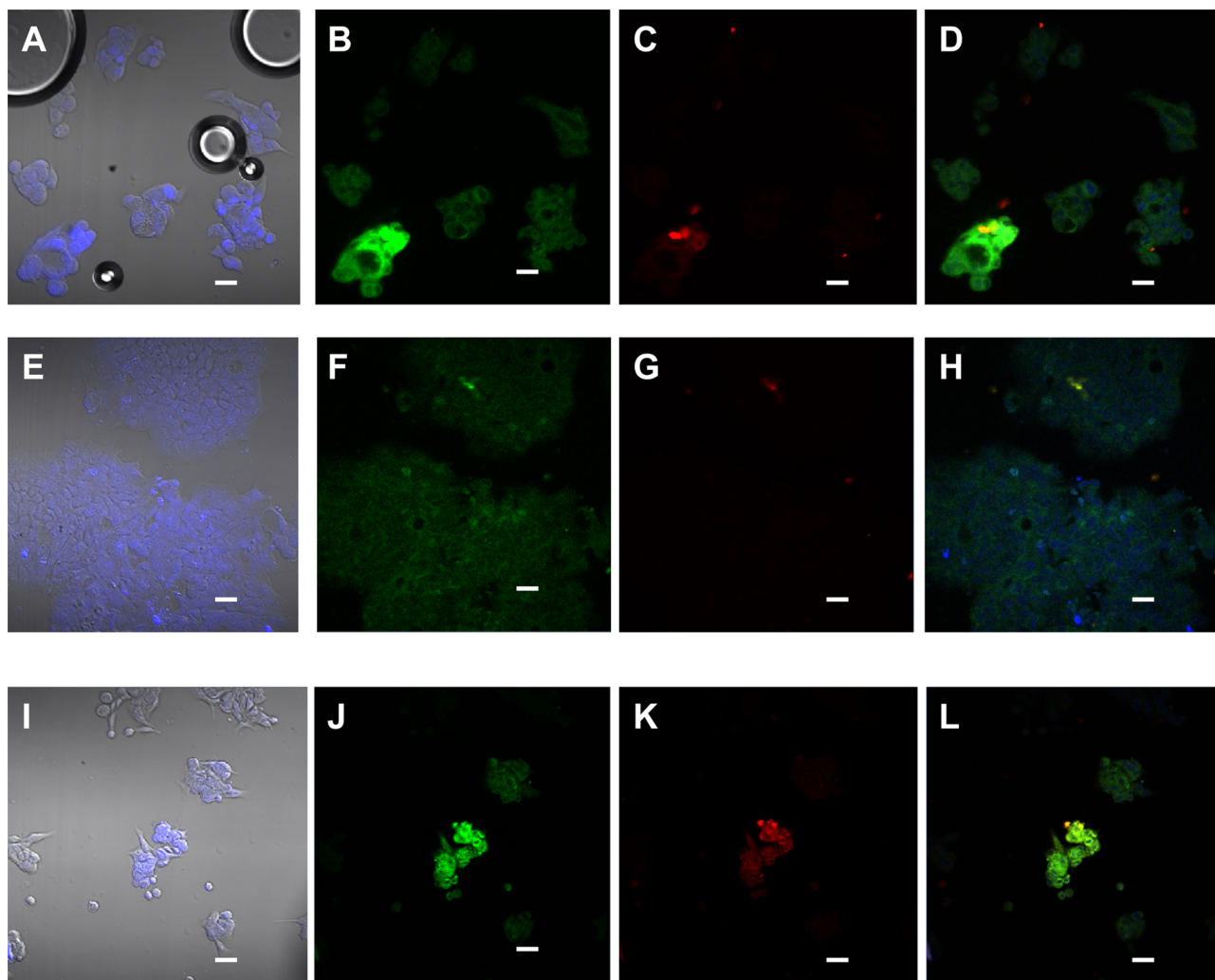


Figure 2. CLSM images of 10 000 LS174T cells with 5 μ g chimeric VLPs (A–L). (A, E, and I) DAPI and overlaid bright-field images. (B, F, and J) BODIPY FL-C5-ceramide complexed to BSA for plasma membrane localization. (C) Alexa594-conjugated anti-DDDDK for rscFVs, (G) Alexa647-conjugated goat antirabbit targeting rabbit anti-M,1 and (K) Alexa647-conjugated goat antirabbit targeting rabbit antigag. (D, H, and L) Overlapped images of all the color channels. Scale bar is 10 μ m.

can transfer both the dye and drug to spheroids, and there was significant penetration, with size ranging between 50–100 μ m.

Testing Vaccination Platform Model. Here, we report the dual use of the nanobiomaterial chimeric VLPs as a platform for vaccination against influenza A virus as proof of concept. Chimeric VLPs composed of gag and M1 protein was suspended in PBS buffer (pH 7.5) and injected into mice in a three-dose regimen with a 2-week interval without any adjuvant. The serum collected 2 weeks after the last dosage was tested by ELISA for its ability to recognize chimera and swine flu-influenza A virus (H1N1). The serum showed specificity for chimera as well as swine flu-influenza A virus (H1N1) (Figure 6A,B). The specificity for the chimeric VLPs was higher, because the serum was polyclonal, thereby showing specificity for other components of chimeric VLPs too. The serum specificity for swine flu as a model showed the dual use of nanobiomaterial as a vaccination platform.

■ DISCUSSION

We prepared a nanobiomaterial with dual function of DDS and vaccination using two capsid proteins, gag-577 and M1, to target tumors and provide immunity against influenza virus

simultaneously in cancer patients. Both proteins are known to oligomerize to form VLPs independently, but here, we report that together they form chimeric VLPs when coexpressed. The coexpression method to produce chimeric VLPs (using coat protein and motifs to display other proteins) have been previously reported.^{10,11} Here, we used a similar approach to produce chimeric VLPs with two coat proteins (M1 and gag-577) displaying different proteins simultaneously (rscFVs and GP64). We have previously shown that GP64 is displayed with ease on VLPs owing to the use of the BmNPV bacmid expression system.^{7,8} Due to the use of a similar expression system, chimera lipid surface was also peppered with GP64 as confirmed by Western blotting. GP64 plays an important role in developing DDS as it facilitates the downstream packaging of chimeric VLPs by assisting in fusion with LUVs by a similar mechanism as reported earlier for VLPs.^{7–9,29}

Here, we explored the effect of M1 and gag-577 on the physical attributes of the chimeric VLPs. According to the TEM images from previous work, an increase in diameter was observed for VLP-hPRR⁷ and VLP-NcSRS2.⁸ The proteins displayed on the surface depending on their molecular weight lead to an increase in diameter (rscFVs < NcSRS2 < hPRR),

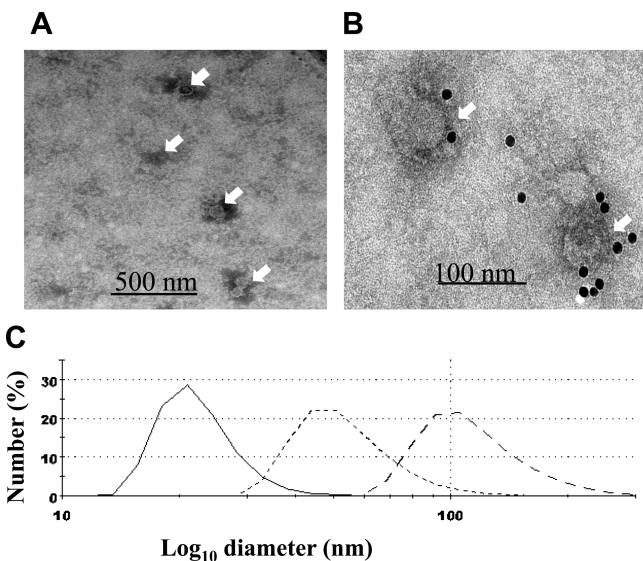


Figure 3. Chimeric VLPs loaded onto carbon grids were negatively stained with 2% (v/v) phosphotungstic acid, as reported earlier.²⁹ (A) TEM, (B) immuno-TEM to confirm rscFvs using primary mouse antibody anti-DYDDDDK and secondary rabbit antimouse conjugated to 10 nm gold particles. (C) One hundred micrograms of chimeric VLPs were resuspended in HEPES buffer, pH 7.5, and the sizes were quantitatively analyzed using dynamic light scattering as reported earlier.²⁹ Solid line: chimera-rscFvs, long dash line: VLP-rscFvs, and short dash line: VLPs. Data are the mean \pm SD ($n = 3$).

because VLPs alone have a smaller diameter. In the case of chimeric VLPs, the displayed protein was rscFvs, which should have given a diameter as observed for VLP-rscFvs, but a more than 50% decrease in diameter was observed, which can be attributed to the presence of M1 (30.5% of total chimeric VLP protein). The changes in the diameter of chimeric VLPs needs

to be further explored to understand how two or more capsid proteins form VLPs. The PyMOL structure alignment (PyMOL Molecular Graphics System, Ver. 1.7.2.1 Schrödinger, LLC.) between gag (PDB: 3TIR) and M1 (PDB: 3DM2) showed that the CA region of gag aligns with M1 with a RMS value of 5.75 Å (Figure S4). The CA region of gag plays an important role in the polymerization of gag, and it has been previously shown that gag protein from HIV-1 can interact with M1 protein from influenza A virus by structure alignments.³²

The size of chimeric VLPs depends on M1, which needs to be further elucidated, but the decrease in diameter does not affect the DDS properties. The decrease in size does not affect the ability of chimeric VLPs to target cancer cells, due to the presence of rscFvs on their surface, and to deliver packaged doxorubicin. Doxorubicin with approximately 10 mg per dosage, depending on the patient's health, is effective as a clinically accepted chemotherapeutic agent^{33–35} but with side effects, which can be controlled with low amount and effective targeted delivery.^{22,36} Chimeric VLPs packaged with doxorubicin have the potential to reduce the harmful side effects by delivering low amounts (13.7 nM) with high specificity to only tumors displaying TAG-72, which needs to be further tested in murine models.

Here, the potential of chimera VLPs as a vaccination platform produced using the bacmid expression system in silkworms was confirmed, as the serum from mice showed specificity for swine flu. The administration of chimeric VLPs to mice required no adjuvant, and like VLPs, they are known to be readily presented to antigen-presenting cells with ease.^{2,28} Because chimeric VLPs are also composed of M1 protein, they can be presented to the antigen-presenting cells and can serve as an alternative platform for vaccine development compared to conservative egg-based or other subunit-based techniques.³⁷ The specificity against other swine flu strains needs to be tested, because the M1-based universal vaccination²⁴ approach has

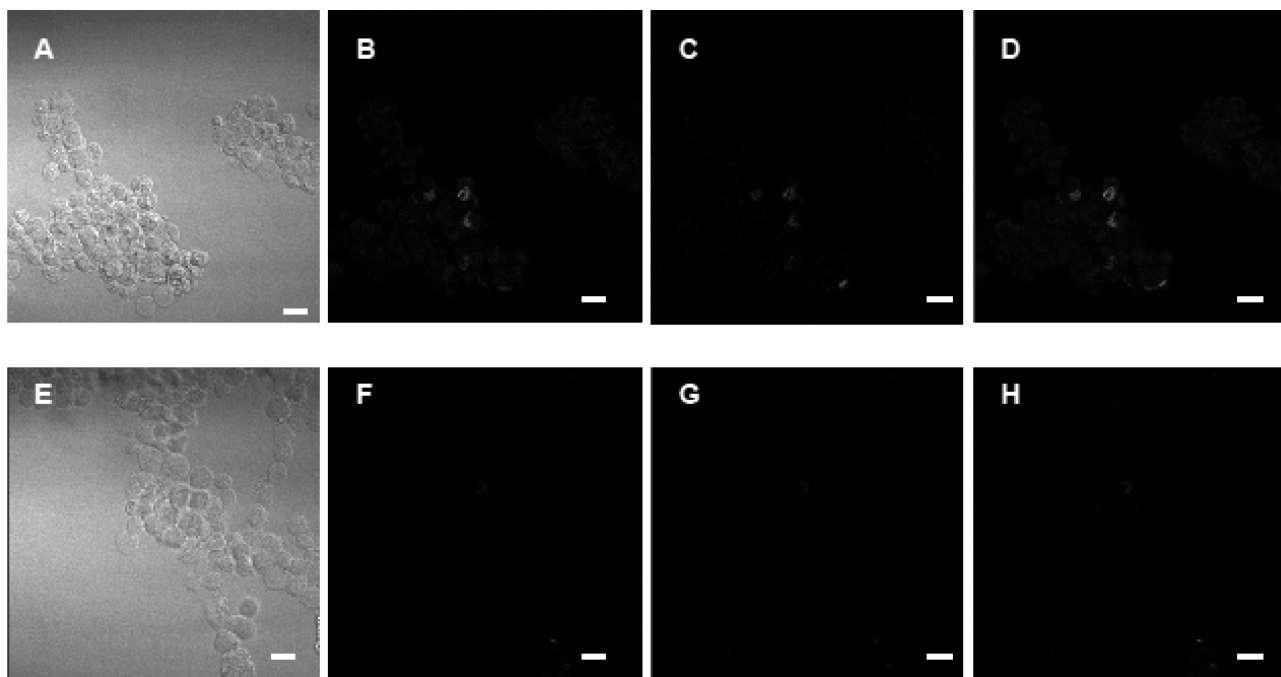


Figure 4. Chimeric VLPs (5 μ g) packaged with LUV-calcein-AM (10 μ M) (A–D) or negative control LUV-calcein-AM (10 μ M) (E–H) were added to 10 000 LS174T cells. (A and E) DIC, (B and F) calcein-AM, (C and G) gag-577 detected using primary antibody rabbit antigag-577 and secondary goat antirabbit-A647, (D and H) merged channels. Scale bar is 10 μ m.

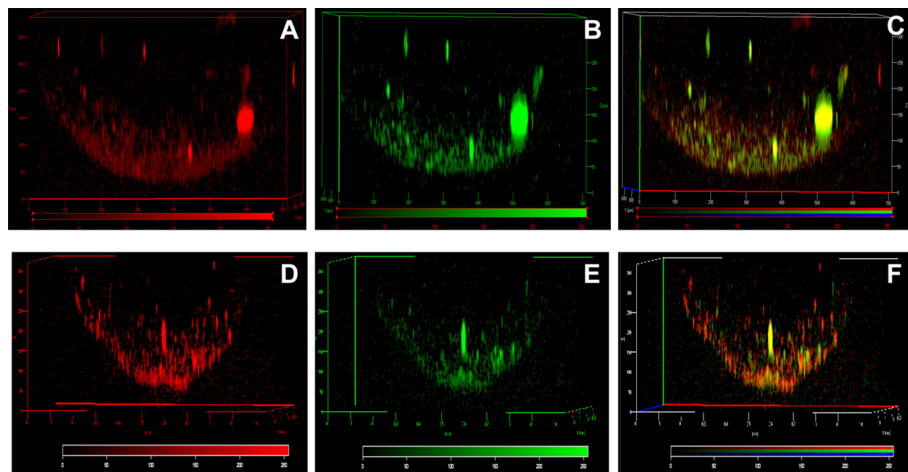


Figure 5. One hundred micrograms of chimeric VLPs packaged with calcein-AM ($10 \mu\text{M}$) (A–C) or doxorubicin (13.7nM) (D–F) were added to large spheroids made using LS174T cells as a model for colon carcinoma. (A) Red fluorescence of calcein-AM, (B, E) green fluorescence of A647 conjugated to rabbit antimouse for mouse anti-DYKDDDDK, (C, F) merged channels and (D) red fluorescence of doxorubicin.

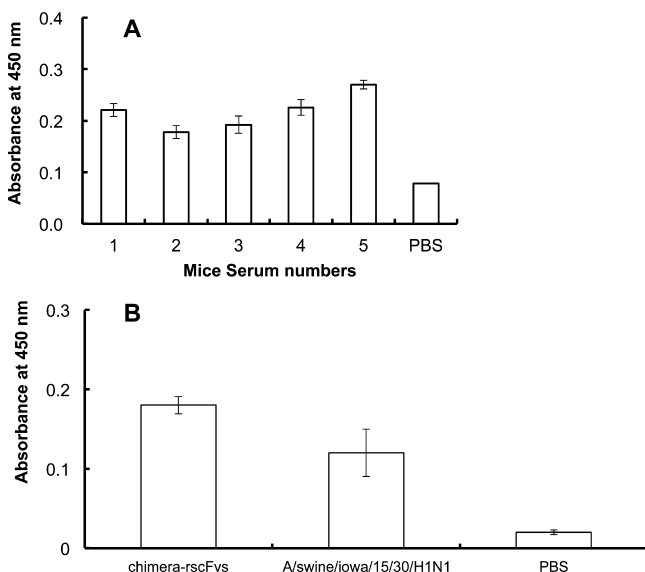


Figure 6. Serum collected from BALB/c mice shows specificity against (A) $5 \mu\text{g}/\text{mL}$ chimera-rscFvs as antigen and (B) one microgram of chimeric VLPs and CEID₅₀ of $10^{6.25}/200 \mu\text{L}$ of A/swine/Iowa/15/30/H1N1 per well immobilized on immunoplate for ELISA. Data are the mean \pm SD ($n = 3$).

produced few successful candidates. The nanobiomaterial reported here can be used for vaccination plus deliver therapeutic drugs to colon tumors. The amount of M1 per microgram of nanobiomaterial needs to be increased to improve the antibody titer, and it needs to be tested further in murine models for DDS (pertaining to penetration) and vaccine development (role in innate and adaptive immune system activation) to further confirm this concept.

■ ASSOCIATED CONTENT

§ Supporting Information

Supplemental data including Western blot analysis of purified chimeric VLPs; CLSM photographs of 10 000 HEK293T and cells with $5 \mu\text{g}$ of chimera VLPs as negative control for specificity; spheroids in 5×7 matrices, which were made using 1.4×10^6 LS174T cells/3D well; and the aligned structures of gag (PDB: 3TIR) and M1 (PDB: 3DM2) by Pymol software.

Experimental details for purification of chimeric VLPs (VLP-M1-rscFv) and Western-blot analysis, LUV preparation and packaging, confirmation of antigen specificity and GPI anchoring of chimera by ELISA, and mouse immunization and mouse serum specificity by ELISA. This material is available free of charge via the Internet at <http://pubs.acs.org>.

■ AUTHOR INFORMATION

Corresponding Author

*E-mail: park.enoch@shizuoka.ac.jp. Tel./Fax: +81-54-238-4887.

Notes

The authors declare no competing financial interest.

■ ACKNOWLEDGMENTS

We thank Prof. Hiroshi Ueda and Prof. Masahito Yamazaki of Tokyo University and Research Institute of Electronics of Shizuoka University for providing the scFv plasmid and calcein-AM. We are grateful to Mr. Takeshi Yamamoto for providing technical assistance in ELISA experiments. This work was supported in part by Promotion of Nanobio-Technology Research to support Aging and Welfare Society from the Ministry of Education, Culture, Sports, Science and Technology, Japan. No additional external funding was received for this study.

■ REFERENCES

- (1) Kang, S.-M. M.; Kim, M.-C. C.; Compans, R. W. Virus-like Particles as Universal Influenza Vaccines. *Expert Rev. Vaccines* **2012**, *11*, 995–1007.
- (2) Roy, P.; Noad, R. Virus-like Particles as a Vaccine Delivery System: Myths and Facts. *Adv. Exp. Med. Biol.* **2009**, *655*, 145–158.
- (3) Raja, K.; Wang, Q.; Gonzalez, M.; Manchester, M.; Johnson, J.; Finn, M. Hybrid Virus–Polymer Materials. 1. Synthesis and Properties of PEG-Decorated Cowpea Mosaic Virus. *Biomacromolecules* **2003**, *4*, 472–476.
- (4) Yu, F.; Joshi, S. M.; Ma, Y. M.; Kingston, R. L.; Simon, M. N.; Vogt, V. M. Characterization of Rous Sarcoma Virus Gag Particles Assembled in Vitro. *J. Virol.* **2001**, *75*, 2753–2764.
- (5) Vogt, V. M.; Simon, M. N. Mass Determination of Rous Sarcoma Virus Virions by Scanning Transmission Electron Microscopy. *J. Virol.* **1999**, *73*, 7050–7055.

- (6) Wills, J. W.; Cameron, C. E.; Wilson, C. B.; Xiang, Y.; Bennett, R. P.; Leis, J. An Assembly Domain of the Rous Sarcoma Virus Gag Protein Required Late in Budding. *J. Virol.* **1994**, *68*, 6605–6618.
- (7) Tsuji, Y.; Deo, V. K.; Kato, T.; Park, E. Y. Production of Rous Sarcoma Virus-like Particles Displaying Human Transmembrane Protein in Silkworm Larvae and Its Application to Ligand-Receptor Binding Assay. *J. Biotechnol.* **2011**, *155*, 185–192.
- (8) Deo, V. K.; Yoshimatsu, K.; Otsuki, T.; Dong, J.; Kato, T.; Park, E. Y. Display of Neospora Caninum Surface Protein Related Sequence 2 on Rous Sarcoma Virus-Derived Gag Protein Virus-like Particles. *J. Biotechnol.* **2013**, *165*, 69–75.
- (9) Deo, V. K.; Tsuji, Y.; Yasuda, T.; Kato, T.; Sakamoto, N.; Suzuki, H.; Park, E. Y. Expression of an RSV-Gag Virus-like Particle in Insect Cell Lines and Silkworm Larvae. *J. Virol. Methods* **2011**, *177*, 147–152.
- (10) Udit, A. K.; Hollingsworth, W.; Choi, K. Metal- and Metallocycle-Binding Sites Engineered into Polyvalent Virus-like Scaffolds. *Bioconjugate Chem.* **2010**, *21*, 399–404.
- (11) Brown, S. D.; Fiedler, J. D.; Finn, M. G. Assembly of Hybrid Bacteriophage Qbeta Virus-like Particles. *Biochemistry* **2009**, *48*, 11155–11157.
- (12) Juarez, V.; Pasolli, A.; Hellwig, A.; Garbi, N.; Arregui, A. Virus-Like Particles Harboring CCL19, IL-2 and HPV16 E7 Elicit Protective T Cell Responses in HLA-A2 Transgenic Mice. *Open Virol. J.* **2012**, *6*, 270–276.
- (13) Fischlechner, M.; Toellner, L.; Messner, P.; Grabherr, R.; Donath, E. Virus - Engineered Colloidal Particles—A Surface Display System. *Angew. Chem., Int. Ed.* **2006**, *45*, 784–789.
- (14) Fesik, S. Promoting Apoptosis as a Strategy for Cancer Drug Discovery. *Nat. Rev. Can.* **2005**, *5*, 876–885.
- (15) Gupta, R.; DuBois, R. Colorectal Cancer Prevention and Treatment by Inhibition of Cyclooxygenase-2. *Nat. Rev. Can.* **2001**, *1*, 11–21.
- (16) Sawyers, C. Targeted Cancer Therapy. *Nature* **2004**, *432*, 294–297.
- (17) Goerner, M.; Seiwert, T.; Sudhoff, H. Molecular Targeted Therapies in Head and Neck Cancer - An Update of Recent Developments -. *Head Neck Oncol.* **2010**, *2*, 8.
- (18) Nishikawa, M. Development of Cell-Specific Targeting Systems for Drugs and Genes. *Biol. Pharm. Bull.* **2005**, *28*, 195–200.
- (19) Agudelo, D.; Bourassa, P.; Bérubé, G.; Tajmir-Riahi, H.-A. Intercalation of Antitumor Drug Doxorubicin and Its Analogue by DNA Duplex: Structural Features and Biological Implications. *Int. J. Biol. Macromol.* **2014**, *66*, 144–150.
- (20) Senavirathna, L.; Fernando, R.; Maples, D.; Zheng, Y.; Polf, J.; Ranjan, A. Tumor Spheroids as an In Vitro Model for Determining the Therapeutic Response to Proton Beam Radiotherapy and Thermally Sensitive Nanocarriers. *Theranostics* **2013**, *3*, 687–691.
- (21) Jiang, X.; Sha, X.; Xin, H.; Xu, X.; Gu, J.; Xia, W.; Chen, S.; Xie, Y.; Chen, L.; Chen, Y.; Fang, X. Integrin-Facilitated Transcytosis for Enhanced Penetration of Advanced Gliomas by Poly(trimethylene Carbonate)-Based Nanoparticles Encapsulating Paclitaxel. *Biomaterials* **2013**, *34*, 2969–79.
- (22) Peer, D.; Karp, J.; Hong, S.; Farokhzad, O.; Margalit, R.; Langer, R. Nanocarriers as an Emerging Platform for Cancer Therapy. *Nat. Nanotechnol.* **2007**, *2*, 751–760.
- (23) Parent, L. New Insights into the Nuclear Localization of Retroviral Gag Proteins. *Nucleus* **2014**, *2*, 92–97.
- (24) Zheng, M.; Luo, J.; Chen, Z. Development of Universal Influenza Vaccines Based on Influenza Virus M and NP Genes. *Infection* **2014**, *42*, 251–262.
- (25) Quan, F.-S.; Kim, M.-C.; Lee, B.-J.; Song, J.-M.; Compans, R.; Kang, S.-M. Influenza M1 VLPs Containing Neuraminidase Induce Heterosubtypic Cross-Protection. *Virology* **2012**, *430*, 127–135.
- (26) Wang, D.; Harmon, A.; Jin, J.; Francis, D.; Christopher-Hennings, J.; Nelson, E.; Montelaro, R.; Li, F. The Lack of an Inherent Membrane Targeting Signal Is Responsible for the Failure of the Matrix (M1) Protein of Influenza A Virus to Bud into Virus-like Particles. *J. of virol.* **2010**, *84*, 4673–4681.
- (27) Latham, T.; Galarza, J. Formation of Wild-Type and Chimeric Influenza Virus-Like Particles Following Simultaneous Expression of Only Four Structural Proteins. *J. Virol.* **2001**, *75*, 6154–6165.
- (28) Noad, R.; Roy, P. Virus-like Particles as Immunogens. *Trends Microbiol.* **2003**, *11*, 438–444.
- (29) Deo, V. K.; Yui, M.; Alam, M. J.; Yamazaki, M.; Kato, T.; Park, E. Y. A Model for Targeting Colon Carcinoma Cells Using Single-Chain Variable Fragments Anchored on Virus-Like Particles via Glycosyl Phosphatidylinositol Anchor. *Pharm. Res.* **2014**, *31*, 2166–2177.
- (30) Kamiya, K.; Kobayashi, J.; Yoshimura, T.; Tsumoto, K. Confocal Microscopic Observation of Fusion between Baculovirus Budded Virus Envelopes and Single Giant Unilamellar Vesicles. *Biochim. Biophys. Acta* **2010**, *1798*, 1625–1631.
- (31) Cho, K.; Shin, H.-W.; Kim, Y.-I.; Cho, C.-H.; Chun, Y.-S.; Kim, T.-Y.; Park, J.-W. Mad1Mediates Hypoxia-Induced Doxorubicin Resistance in Colon Cancer Cells by Inhibiting Mitochondrial Function. *Free Radical Biol. Med.* **2013**, *60*, 201–210.
- (32) Harris, A.; Sha, B.; Luo, M. Structural Similarities between Influenza Virus Matrix Protein M1 and Human Immunodeficiency Virus Matrix and Capsid Proteins: An Evolutionary Link between Negative-Stranded RNA Viruses and Retroviruses. *J. Gen. Virol.* **1999**, *80*, 863–869.
- (33) Laginha, K.; Verwoert, S.; Charrois, G.; Allen, T. Determination of Doxorubicin Levels in Whole Tumor and Tumor Nuclei in Murine Breast Cancer Tumors. *Clin. Cancer Res.* **2005**, *11*, 6944–6949.
- (34) Russell, S.; Blackwell, K.; Lawrence, J.; Pippen, J.; Roe, M.; Wood, F.; Paton, V.; Holmgren, E.; Mahaffey, K. Independent Adjudication of Symptomatic Heart Failure With the Use of Doxorubicin and Cyclophosphamide Followed by Trastuzumab Adjuvant Therapy: A Combined Review of Cardiac Data From the National Surgical Adjuvant Breast and Bowel Project B-31 and the North Central Cancer Treatment Group N9831 Clinical Trials. *J. Clin. Oncol.* **2010**, *28*, 3416–3421.
- (35) Main, C.; Bojke, L.; Griffin, S.; Norman, G.; Barbieri, M.; Mather, L.; Stark, D.; Palmer, S.; Riemsma, R. Topotecan, Pegylated Liposomal Doxorubicin Hydrochloride and Paclitaxel for Second-Line or Subsequent Treatment of Advanced Ovarian Cancer: A Systematic Review and Economic Evaluation. *Health Technol. Assess.* **2006**, *10*, 1–132.
- (36) Peer, D.; Margalit, R. Tumor-Targeted Hyaluronan Nanoliposomes Increase the Antitumor Activity of Liposomal Doxorubicin in Syngeneic and Human Xenograft Mouse Tumor Models. *Neoplasia* **2004**, *6*, 343–353.
- (37) Grgacic, E.; Anderson, D. Virus-like Particles: Passport to Immune Recognition. *Methods* **2006**, *40*, 60–65.